doi:10.1093/brain/awl174 *Brain* (2006), **129**, 2103–2118

Early onset severe and late-onset mild Charcot–Marie–Tooth disease with mitofusin 2 (*MFN2*) mutations

K. W. Chung,[1] S. B. Kim,[2] K. D. Park,[3] K. G. Choi,[3] J. H. Lee,[4] H. W. Eun,[5] J. S. Suh,[5] J. H. Hwang,[1] W. K. Kim,[6] B. C. Seo,[7] S. H. Kim,[8] I. H. Son,[9] S. M. Kim,[7] I. N. Sunwoo[7] and B. O. Choi[3]

[1]Department of Biological Science, Kongju National University, Kongju, [2]Department of Neurology, Kyung Hee University, College of Medicine, Departments of [3]Neurology, [4]Ophthalmology, [5]Radiology and Ewha Medical Research Center, [6]Division of Nanosciences, Ewha Woman's University, College of Medicine, Departments of [7]Neurology and [8]Pathology, Yonsei University College of Medicine, Seoul and [9]Department of Neurology and INAM Neuroscience Research Center, Wonkwang University, College of Medicine, Gunpo, Korea

Correspondence to: Prof. Byung-Ok Choi, MD, PhD, Department of Neurology and Ewha Medical Research Center, Ewha Woman's University, College of Medicine, Dongdaemun Hospital, 70 Jongno 6-ga, Jongno-gu, 110-783, Seoul, Korea
E-mail: bochoi@ewha.ac.kr

Mutations in the mitofusin 2 (*MFN2*) gene, which encodes a mitochondrial GTPase mitofusin protein, have recently been reported to cause both Charcot–Marie–Tooth 2A (CMT2A) and hereditary motor and sensory neuropathy VI (HMSN VI). It is well known that HMSN VI is an axonal CMT neuropathy with optic atrophy. However, the differences between CMT2A and HMSN VI with *MFN2* mutations remained to be clarified. Therefore, we studied the phenotypic characteristics of CMT patients with *MFN2* mutations. Mutations in *MFN2* were screened in 62 unrelated axonal CMT neuropathy families. We calculated CMT neuropathy scores (CMTNSs) and functional disability scales (FDSs) to quantify disease severity. Twenty-one patients with the *MFN2* mutations were studied by brain MRI. Ten pathogenic mutations were identified in 26 patients from 15 families (24.2%). Six of these mutations had not been reported, and *de novo* mutations were observed in five families (33.3%). The electrophysiological patterns of affected individuals with the *MFN2* mutations were typical of axonal CMT; however, the clinical and electrophysiological characteristics were markedly different in early (<10 years) and late disease-onset (≥10 years) groups. All patients with an early onset had severe CMTNS (≥21) and FDS (6 or 7), whereas most patients with late onset had mild CMTNS (≤10) and FDS (≤3). We identified two HMSN VI families with the R364W mutation in the early onset group; however, two other families with the same mutation did not have optic atrophy. In addition, two early onset families with R94W mutations, previously reported for HMSN VI, did not have visual impairment. Interestingly, eight patients had periventricular and subcortical hyperintense lesions by brain MRI. In the late-onset group, three patients had sensorineural hearing loss and two had bilateral extensor plantar responses. We found that *MFN2* mutations are the major cause of axonal CMT neuropathy, and that they are associated with variable CNS involvements. Phenotypes were significantly different in the early and late disease-onset groups. Our findings suggest that HMSN VI might be a variant of the early onset severe CMT2A phenotype.

Keywords: Charcot–Marie–Tooth disease; CMT2A; HMSN VI; mitofusin 2 (*MFN2*)

Abbreviations: CMAP = compound muscle action potential; CMT = Charcot–Marie–Tooth; CMTNS = CMT neuropathy score; FDS = functional disability scale; FLAIR = fluid-attenuated inversion recovery; HMSN = hereditary motor and sensory neuropathy; MCV = motor nerve conduction velocity; *MFN2* = mitofusin 2; MNF = myelinated nerve fibre; MRC = Medical Research Council; PCR = polymerase chain reaction; SCV = sensory nerve conduction velocity; SNAP = sensory nerve action potential; SNHL = sensorineural hearing loss; TLIs = terminal latency indices; VEP = visual evoked potential

Received April 12, 2006. Revised May 31, 2006. Accepted June 7, 2006. Advance Access publication July 10, 2006

Introduction

Charcot–Marie–Tooth (CMT) disease is a genetically and clinically heterogeneous disorder, and many CMT-causative genes have been identified (Shy *et al.*, 2004). CMT is frequently classified as type 1, the demyelinating form (CMT1), or type 2, the axonal form (CMT2). The primary defect in CMT2 patients is neuronal, and CMT2 patients have slightly reduced (>38 m/s) or even normal nerve conduction velocities (NCVs) (Pareyson *et al.*, 2004).

CMT2 has been divided into many subtypes by linkage analysis as follows: CMT2A (1p35–p36), 2B (3q21), 2D (7p15), 2E (8p21), 2F (7q11.23), 2G (12q12–q13.3), 2I (1q22), 2K (8q13–q21.1) and 2L (12q24). Several genes have been reported to be associated with CMT2 loci, namely, kinesin family member 1B-β (*KIF1B*: MIM no. 605995) in CMT2A (Zhao *et al.*, 2001), *RAB7* (MIM no. 602298) in CMT2B (Verhoeven *et al.*, 2003), *GARS* (MIM no. 600287) in CMT2D (Antonellis *et al.*, 2003), *NEFL* (MIM no. 162280) in CMT2E (Mersiyanova *et al.*, 2000; Choi *et al.*, 2004), *HSPB1* (MIM no. 602195) in CMT2F (Evgrafov *et al.*, 2004), *MPZ* (MIM no. 159440) in CMT2I (Boerkoel *et al.*, 2002) and *HSPB8* (MIM no. 608014) in CMT2L (Tang *et al.*, 2005).

Following the mapping of CMT2A to the short arm of chromosome 1, 1p35–p36, a missense mutation was detected in *KIF1B* in a Japanese CMT2A family (Zhao *et al.*, 2001). However, no other mutation has been identified in *KIF1B*, and, thus, it is believed that another gene is involved (Muglia *et al.*, 2001; Bissar-Tadmouri *et al.*, 2004). By linkage analysis and screening genes linked to the CMT2A locus, Züchner *et al.* (2004) first identified several mutations in the mitofusin 2 (*MFN2*) gene. Subsequently, additional *MFN2* mutations were reported in CMT2A patients (Kijima *et al.*, 2005; Lawson *et al.*, 2005). Thus, today, mutations in *MFN2* are considered to provide the genetic basis of the CMT2A phenotype. *MFN2* encodes an outer mitochondrial membrane protein, which has important roles in the regulation of the fusion of mitochondria in cooperation with the Mfn1 isoform (Rojo *et al.*, 2002; Chen *et al.*, 2003; Koshiba *et al.*, 2004). Mitochondrial fusion is essential for various biological functions in eukaryotic cells (Chen *et al.*, 2005). It has also been suggested that *MFN2* may be associated with the maintenance of mitochondrial membrane potentials (Honda *et al.*, 2005). Moreover, *MFN2*-deficient mice die in mid-gestation and display fragmented mitochondria (Chen *et al.*, 2003). In addition, it is believed, even in a few population-based studies, that *MFN2* mutations are most common in CMT2 (Szigeti *et al.*, 2006).

Recently, axonal CMT neuropathy with visual impairment due to optic atrophy designated as hereditary motor and sensory neuropathy type VI (HMSN VI) was also shown to be caused by mutations in the *MFN2* gene (Züchner *et al.*, 2006). After the vertical inheritance in HMSN VI from male to male was first documented by Vizioli (1889), other patterns of inheritance have been demonstrated, that is, autosomal dominant with incomplete penetrance (Voo *et al.*, 2003; Züchner *et al.*, 2006), autosomal recessive (Schneider and Abeles, 1937; Iwashita *et al.*, 1970), X-linked recessive (Rosenberg and Chutorian, 1967) and sporadic (Krauss, 1906). These variable inheritance patterns of HMSN VI may be due to the incomplete penetrance of optic atrophy.

Because *MFN2* mutation screening studies and examinations of the relationships between genotypes and clinical phenotypes have only been performed recently in CMT patients, mutation data in different ethnic groups are limited (Kijima *et al.*, 2005; Lawson *et al.*, 2005). Therefore, we screened for *MFN2* mutations in 62 unrelated axonal CMT neuropathy families and identified 10 causative mutations in 15 families. We found that some affected individuals developed unusually severe phenotypes with an early onset and others a mild form of axonal neuropathy with a late age of onset. In addition, we detected two HMSN VI families with the R364W *MFN2* mutation; however, the other two families with the same mutations did not show optic atrophy.

Patients and methods

Patients

This study included a total of 218 patients from 62 families with distinct CMT type 2 phenotypes of Korean origin. Blood samples were collected from patients diagnosed as having CMT at Ewha Woman's University Hospital. The clinical guidelines of the European CMT consortium were used to diagnose CMT type 2 (De Jonghe *et al.*, 1998). In addition, 200 healthy controls for sequence variations were recruited from the neurological department, after careful clinical and electrophysiological examinations. In families with *de novo* mutation, paternity and maternity were confirmed in these families by genotyping 15 markers provided in AmpFLSTR identifier kits (Applied Biosystems, Foster City, CA, USA). All participants included in this study provided written informed consent according to the protocol approved by the Ethics Committee of Ewha Woman's University Hospital.

MFN2 mutation screening

DNA was extracted from blood samples using a genomic DNA isolation kit (SolGent, Daejeon, Korea). All exons of *MFN2* were amplified using a standard polymerase chain reaction (PCR) method. Exons 7–8, 10–11 and 13–14 were amplified together, whereas the others were amplified separately. The primer sequences and PCR conditions used are available on request. PCR products were purified using PCR product purification kits (SolGent, Daejeon, Korea) and sequenced using an ABI 3100 automatic sequencer (Applied Biosystems-Hitachi, Tokyo, Japan). Sequence variations were confirmed by analysing both DNA strands.

Clinical assessment

Clinical information was obtained in a standardized manner and included assessments of motor and sensory impairments, deep tendon reflexes and muscle atrophy. Muscle strengths of flexor and extensor muscles were assessed manually using the standard Medical Research Council (MRC) scale. In order to determine physical disability, we used two scales, a functional disability scale (FDS)

(Birouk *et al.*, 1998) and a CMT neuropathy score (CMTNS) (Shy *et al.*, 2005). Disease severity was determined for each patient using a nine-point FDS, which was based on the following criteria: 0 = normal; 1 = normal but with cramps and fatigability; 2 = an inability to run; 3 = walking difficulty but still possible unaided; 4 = walking with a cane; 5 = walking with crutches; 6 = walking with a walker; 7 = wheelchair-bound; and 8 = bedridden. In addition, we determined the recently created CMTNS, based on motor and sensory symptoms, and on pain and vibration, muscle strength and neurophysiological test results. Moreover, patients were divided into mild (CMTNS $\leqslant$ 10), moderate (CMTNS $\geqslant$11 and $\leqslant$20) and severe (CMTNS $\geqslant$ 21) categories. Sensory impairments were assessed in terms of the level and severity of pain, temperature, vibration and position, and pain and vibration sense were compared. Age at onset was determined by asking patients for their ages, when symptoms, that is, distal muscle weakness, foot deformity or sensory change, first appeared. Ophthalmological examination, done in all patients with *MFN2* mutations, included best-corrected visual acuity, colour vision using Ishihara colour plates, pupillary reflex, automated visual field test, anterior segment and dilated fundus examination.

Electrophysiological study

Motor and sensory conduction velocities of median, ulnar, peroneal, tibial and sural nerves were determined in 26 patients. Recordings were obtained by standard methods using surface stimulation and recording electrodes. Motor conduction velocities (MCVs) of the median and ulnar nerves were determined by stimulating at the elbow and wrist while recording compound muscle action potentials (CMAPs) over the abductor pollicis brevis and abductor digiti quinti, respectively. In the same way, the MCVs of peroneal and tibial nerves were determined by stimulating at the knee and ankle, while recording CMAPs over the extensor digitorum brevis and abductor hallucis, respectively. CMAP amplitudes were measured from positive peak to negative peak values. Sensory conduction velocities (SCVs) were obtained over a finger-wrist segment from the median and ulnar nerves by orthodromic scoring and were also recorded for sural nerves. Sensory nerve action potential (SNAP) amplitudes were measured from positive peaks to negative peaks. Terminal latency indices (TLIs) were calculated for median nerves [TLI = terminal distance (mm)/MCV (m/s) $\times$ distal motor latency (ms)].

MRI study

Twenty-one individuals with *MFN2* mutations were evaluated using a 1.5-T system (Siemens Vision; Siemens, Erlangen, Germany). Whole brains were scanned using a slice thickness of 7 mm and a 2-mm interslice gap, to produce 16 axial images. The imaging protocol consisted of T_2-weighted spin echo [repetition time (TR)/echo time (TE) = 4700/120 ms], T_1-weighted spin echo (TR/TE = 550/12 ms) and fluid-attenuated inversion recovery (FLAIR) (TR/TE = 9000/119 ms, inversion time 2609 ms) images.

Histopathological study

Pathological examinations of affected individuals included the light and electron microscopic analyses of a sural nerve. One sural nerve fragment was fixed in 10% formalin, embedded in paraffin and stained with haematoxylin–eosin (H–E). Another fragment was immediately fixed by immersion in 5% buffered glutaraldehyde and post-fixed in 1% osmium tetroxide. Epon-embedded semi-thin and ultra-thin sections were prepared for light and ultra-structural examinations. In addition, a muscle biopsy was taken from the gastrocnemius under local anaesthesia. Cross-sections of biopsy tissue were stained with H–E, modified Gomori-trichrome and oxidative enzymes (NADH-TR, succinate dehydrogenase). Another biopsy fragment was examined by electron microscopy.

Statistical analysis

Percentages and means were compared using the χ^2-test and the Student's *t*-test, respectively. Correlation studies were performed using Spearman's correlation coefficient (*r*), and strong correlations were considered significant when *r*-values were >0.7 and *P*-values were <0.05. Statistical significance was accepted for *P*-values exceeding 0.05. Statistical analyses were performed using SPSS for Windows, Ver. 11.0 (SPSS Inc., Chicago, IL, USA).

Results

Identification of causative mutations

Mutation screening of *MFN2* in 62 unrelated CMT2 families identified ten causative missense mutations in 15 families (24.2%). Details of the mutations are listed in Table 1. Most mutations were located within or close to the GTPase domain. Six mutations [c.275T→C (L92P), c.380G→A (G127D), c.494A→G (H165R), c.787T→C (S263P), c.1085C→T (T362M) and c.1127T→C (M376T)] had not been reported previously, and were not detected in the 400 control chromosomes (Fig. 1A). Amino acid sequences are highly conserved in different species at most mutation sites (Fig. 1B). In the present study, CMT2A families with *MFN2* mutations showed an autosomal dominant inheritance, even though there were *de novo* mutations. Five *de novo* mutations were proved in 5 families of the 15 CMT2A families (33.3%), which is a high rate.

The c.275T→C (L92P) *de novo* mutation at exon 4 was found in a patient with a severe CMT2 phenotype (FC34). This mutation was only detected in the proband (III-2), who was the only affected member of his family (Fig. 2A). The c.280C→T (R94W) autosomal dominant mutation at exon 4 was detected in severely affected individuals of two CMT2 families. This mutation was transmitted from father (possible affected) to son in Family FC25 (Fig. 2B) and from mother to son in Family FC113 (Fig. 2C), respectively. Mutations at the 94th codon have been previously reported in several families (Züchner *et al.*, 2004; Kijima *et al.*, 2005). Two *de novo* mutations at exon 5, c.314C→T (T105M) and c.380G→A (G127D), were identified in CMT2 families with a mild phenotype, FC135 (Fig. 2D) and FC48 (Fig. 2E), respectively. The T105M mutation has been previously reported in two CMT2 families (Züchner *et al.*, 2004; Lawson *et al.*, 2005). The c.494A→G (H165R) mutation at exon 6 was detected in two CMT2 families with a mild phenotype, FC81 (Fig. 2F) and FC111 (Fig. 2G). This mutation co-segregated to affected members in both pedigrees in an autosomal dominant mode. The exon 8 c.787T→C (S263P) mutation was identified in a mild CMT2 family (FC52) and had been transmitted from mother to son

Table 1 Mutations found in the *MFN2* gene in Korean pedigrees

Exon	Domain	Nucleotide change	Amino acid change	Index family	Inheritance	Phenotype	Reference
Exon 4		c.275T→C	p.L92P	FC34	*De novo*	Early onset, severe	This study
Exon 4		c.280C→T	p.R94W	FC25	AD	Early onset, severe	Züchner *et al.*, 2004, 2006;
				FC113	AD	Early onset, severe	Kijima *et al.*, 2005
Exon 5	GTPase	c.314C→T	p.T105M	FC135	*De novo*	Late onset, mild	Züchner *et al.*, 2004; Lawson *et al.*, 2005
Exon 5	GTPase	c.380G→A	p.G127D	FC48	*De novo*	Late onset, mild	This study
Exon 6	GTPase	c.494A→G	p.H165R	FC81	AD	Late onset, mild	This study
				FC111	AD	Late onset, mild	
Exon 8		c.787T→C	p.S263P	FC52	AD	Late onset, mild	This study
Exon 9		c.839G→A	p.R280H	FC169	AD	Late onset, mild	Züchner *et al.*, 2004
Exon 11		c.1085C→T	p.T362M	FC188	AD	Late onset, mild	This study
Exon 11		c.1090C→T	p.R364W	FC1	AD (*De novo*)	Early onset, severe	Züchner *et al.*, 2006
				FC6	AD	Early onset, severe	
				FC55	*De novo*	Early onset, severe	
				FC87	AD	Early onset, severe	
Exon 11		c.1127T→C	p.M376T	FC70	AD	Late onset, mild	This study

Nucleotide numbering: the first nt 'A' of the ATG translation start codon is designated +1.
Reference sequence accession number of *MFN2* is NM 014874.
AD = autosomal dominant inheritance.

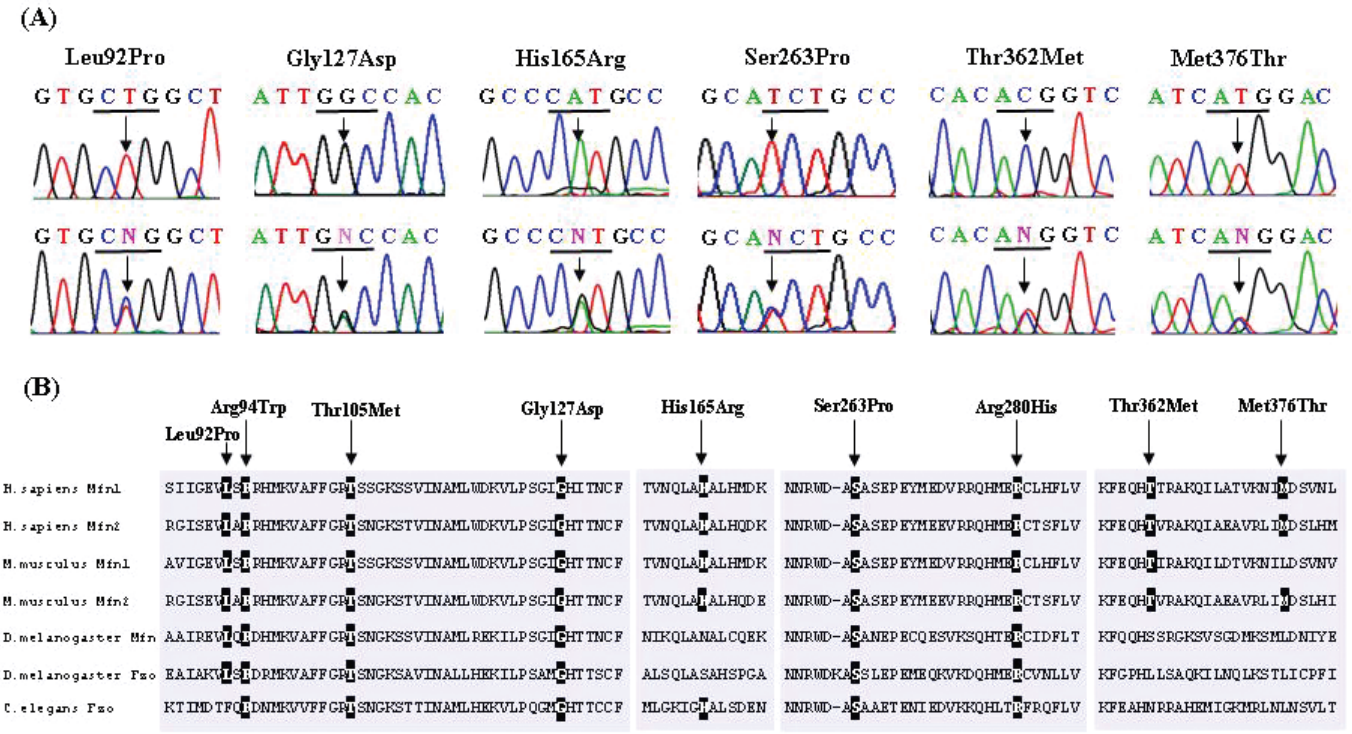

Fig. 1 *MFN2* mutations and their conservation in species. (**A**) Chromatograms of six novel mutations. Exons were amplified by standard PCR and sequenced using an ABI 3100 automatic sequencer (Applied Biosystems-Hitachi, Tokyo, Japan). (**B**) Conservation of amino acids at mutation sites in different species. Mutation sites are indicated by arrows.

(Fig. 2H), and c.839G→A (R280H), an autosomal dominant mutation at exon 9, was also identified in a mild CMT2 family, FC169 (Fig. 2I). The R280H mutation has been previously reported in a CMT2 family (Züchner *et al.*, 2004). A novel c.1085C→T (T362M) mutation was observed in a late-onset CMT2 family with a mild phenotype (FC188). The proband (II-2) had received the mutation from her mother (I-2), who showed very mild phenotype (Fig. 2J). Four families with a severe phenotype were found to possess c.1090C→T (R364W) at exon 11. In the FC1 pedigree (Fig. 2K), the proband (III-1) and her twin sister (III-2) had received the mutation from their mother (II-3),

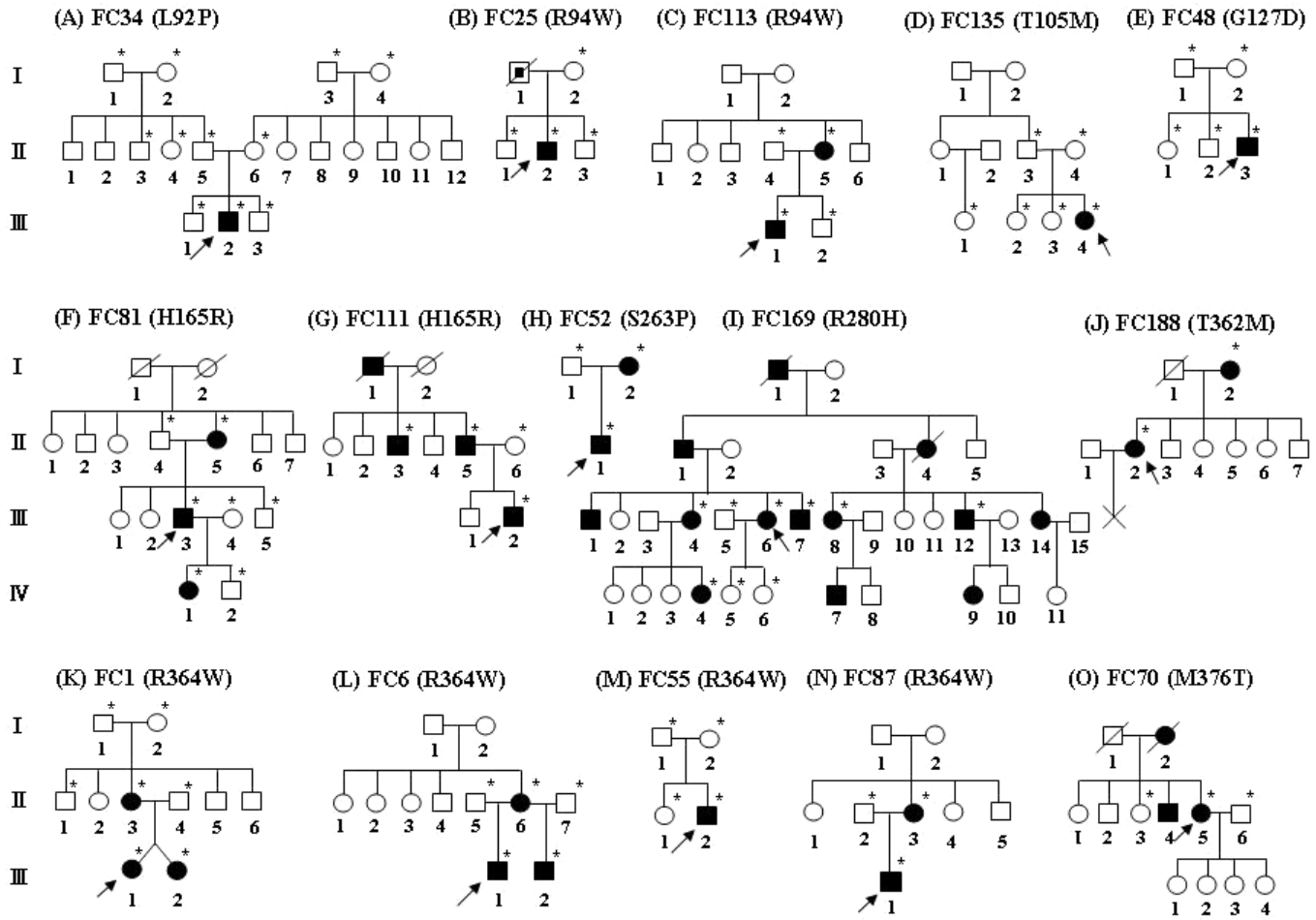

Fig. 2 Pedigrees of CMT2A families with *MFN2* mutation. The available DNA samples are indicated by asterisks (*). The open symbols represent unaffected males (open squares) and unaffected females (open circles), and filled symbols represent affected males (closed squares) and affected females (closed circles). The half-filled symbol indicates a possible affected male. The arrows indicate probands. (**A**) FC34 with L92P, (**B**) FC25 with R94W, (**C**) FC113 with R94W, (**D**) FC135 with T105M, (**E**) FC48 with G127D, (**F**) FC81 with H165R, (**G**) FC111 with H165R, (**H**) FC52 with S263P, (**I**) FC169 with R280H, (**J**) FC188 with T362M, (**K**) FC1 with R364W, (**L**) FC6 with R364W, (**M**) FC55 with R364W, (**N**) FC87 with R364W and (**O**) FC70 with M376T.

but II-3 was a *de novo* case. FC6 (Fig. 2L) and FC87 (Fig. 2N) showed autosomal dominant inheritance (mother to son), whereas FC55 (Fig. 2M) showed a *de novo* mutation. The c.1127T→C (M376T) autosomal dominant mutation at exon 11 was identified in mild patients in a CMT2 pedigree (FC70; Fig. 2O). This mutation had been transmitted from mother (I-2) to the proband (II-5) and her brother (II-4).

We also found several polymorphic variants in the exon region: c.–212T→C (5′-UTR, exon 1), c.150C→A (I150I), c.165C→T (T55T), c.408A→T (V136V), c.1569C→T (S523S) and c.2332A→G (3′-UTR at exon 19). These variants were also observed in controls, but no amino acid substitutions were involved; thus, they were not regarded as causative mutations. Some polymorphic sites (c.150C→A, c.165C→T, c.408A→T and c.1569C→T) have been reported previously (Kijima *et al.*, 2005). A mutation at intron 5 near the 5′-splicing site, c.474+4A→G, was also detected in two CMT2 families. However, this mutation did not co-segregate to affected individuals and was also found in controls at a frequency of 0.015, and, thus, was not considered a causative mutation.

Clinical findings

The clinical features of the 26 patients (11 males, 15 females) from the 15 families are shown in Table 2. Muscle weakness and atrophy started and predominated in the distal portions of legs and were noted to a lesser extent distally in upper limbs. Paresis in the distal regions of lower limbs varied from asymptomatic or mild weakness to the complete paralysis of distal muscle groups.

Age at onset was earlier than 10 years (early onset group) in five males and seven females and occurred later (late-onset group) in six males and eight females. Mean age at onset was 3.9 ± 3.0 years (range: 1–9 years) in the early onset group and 23.9 ± 13.0 years (range: 10–50 years) in

Table 2 Clinical features in 26 CMT patients from 15 families with *MFN2* mutations

Patients	Sex	Age at exam (years)	Age at onset (years)	Disease duration (years)	FDS	CMTNS	Muscle weakness[a]		Muscle atrophy[b]	Sensory loss[c]		DTR[d]		Additional symptoms	Pathological findings
							U/E	L/E		U/E	L/E	U/E	L/E		
Early age at onset (<10 years)															
FC1 (II-3)	F	35	8	27	7	36	++	+++	Severe (U < L)	P = V	P = V	A	A	Scoliosis, contracture optic atrophy	Sural nerve, axonal, pseudo-onion bulb
FC1 (III-1)	F	12	1	11	7	36	++	+++	Severe (U < L)	P = V	P = V	A	A	Scoliosis, contracture	ND[e]
FC1 (III-2)	F	12	1	11	7	36	++	+++	Severe (U < L)	P = V	P < V	A	A	Scoliosis, contracture	ND
FC6 (II-6)	F	33	5	28	7	36	++	+++	Severe (U < L)	P < V	P < V	A	A	Scoliosis, contracture hoarseness, optic atrophy	Sural nerve, axonal
FC6 (III-1)	M	14	2	12	7	34	++	+++	Severe (U < L)	P < V	P < V	A	A	Scoliosis, contracture, optic atrophy	ND
FC25 (II-2)	M	28	9	19	6	22	++	+++	Severe (U < L)	P = V	P = V	A	A	–	ND
FC34 (III-2)	M	13	1	12	6	31	++	+++	Severe (U < L)	P = V	P < V	A	A	Scoliosis	Sural nerve, axonal
FC55 (II-2)	F	6	3	3	6	31	++	+++	Severe (U < L)	P = V	P < V	A	A	Scoliosis	ND
FC87 (II-3)	F	22	4	18	7	36	++	+++	Severe (U < L)	P < V	P < V	A	A	Scoliosis, contracture	Sural nerve, axonal
FC87 (III-1)	M	3	1	2	6	28	++	+++	Severe (U < L)	ND	ND	A	A	–	ND
FC113 (II-5)	F	37	8	29	7	33	++	+++	Severe (U < L)	P < V	P < V	A	A	Scoliosis, contracture	Sural nerve, axonal
FC113 (III-1)	M	6	4	2	6	22	+	+++	Severe (U < L)	P < V	P < V	A	A	Scoliosis	ND
Late age at onset (⩾10 years)															
FC48 (II-3)	M	26	16	10	2	4	–	+	No	nl	P > V	N	I	Extensor plantar responses	ND
FC52 (II-1)	M	14	12	2	1	5	–	+	Mild (L)	P = V	P = V	D	D	–	ND
FC70 (II-5)	F	53	39	14	2	10	+	++	Mild (U < L)	P = V	P = V	D	A	Pain	ND
FC81 (II-5)	F	64	50	14	1	5	–	–	No	P = V	P = V	N	D	Tremor, SNHL	Sural nerve, axonal
FC81 (III-3)	M	35	10	25	3	15	+	++	Mild (U < L)	P = V	P > V	N	A	Tremor, SNHL, hoarseness	ND
FC111 (III-2)	M	20	14	6	1	5	–	+	No	P = V	P = V	N	D	–	ND
FC135(III-4)	F	12	11	1	2	6	+	++	Mild (L)	P = V	P = V	D	A	Tremor	Gastrocnemius muscle, no RRF
FC169 (III-4)	F	45	23	22	1	6	+	++	Mild (L)	P > V	P > V	N	D	Pain, tremor, dysarthria, migraine	ND
FC169 (III-6)	F	40	34	6	1	7	–	+	No	P = V	P = V	N	D	Tremor	ND
FC169 (III-7)	M	37	27	10	0	2	–	+	No	nl	nl	N	I	Extensor plantar responses	ND
FC169 (III-8)	F	52	25	27	1	8	+	+	No	P = V	P = V	N	D	Pain, tremor, dysarthria, migraine	ND
FC169 (III-12)	M	38	20	18	2	9	–	+	Mild (L)	nl	P = V	N	N	Pain, tremor, SNHL	ND
FC169 (IV-4)	F	14	11	3	2	10	+	++	Mild (L)	P = V	P = V	N	D	Pain, tremor	ND
FC188 (II-2)	F	49	42	7	1	7	–	+	Mild (L)	P = V	P = V	N	D	Transient sensory loss	Sural nerve, axonal

[a]Muscle weakness in lower limbs: + = ankle dorsiflexion 4/5 on MRC scale; ++ = ankle dorsiflexion <4/5 on MRC scale; +++ = proximal weakness and wheelchair-dependent. Muscle weakness in upper limbs: + = intrinsic hand weakness 4/5 on MRC scale; ++ = intrinsic hand weakness <4/5 on MRC scale; – = no symptoms.
[b]Muscle atrophy: U < L = lower limb predominant muscle atrophy; L = only lower limb muscle atrophy. [c]Sensory loss: P = pain sense; V = vibration sense; nl = normal sense.
[d]Deep tendon reflexes: N = normal; D = diminished; A = absent. [e]ND = not done.

late-onset group ($P < 0.001$). Disease duration at the time of examination was 14.5 ± 9.8 years in the early onset group and 11.8 ± 8.5 years in the late-onset group, which was not significantly different. Clinical findings confirmed that patients in the early onset group were more severely affected than those in the late-onset group, and this was significant for several items, that is, severity of muscle weakness ($P < 0.01$), frequency of upper and lower limb areflexia ($P < 0.01$) and the presence of flat feet deformities ($P < 0.01$). Length-dependent sensory loss was found in 24 patients (92.3%). Vibration sense was reduced to a greater extent than pain in 8 of the 12 patients in the early onset group (66.7%). In the late-onset group, pain sense was reduced to a greater extent than vibration in 3 of 14 patients (21.4%), whilst in 10 patients (71.4%) those were reduced to a similar extent.

Functional disability was severe in patients with an early onset, but mild in patients with a late onset. Mean FDS was 6.6 ± 0.5 in the early onset group and 1.4 ± 0.8 in late-onset group ($P < 0.001$). CMTNS was 31.8 ± 5.2 in the early onset group and 7.1 ± 3.2 in the late-onset group, which was significantly different ($P < 0.001$). High FDSs (score = 6 or 7) were found only in the early onset group; however, the late-onset group members showed low FDSs (score ⩽ 3). All 12 patients in the early onset group were in the severe (CMTNS ⩾ 21) category. Except for one patient (III-3 in Family FC81; CMTNS = 15), who was in moderate category, 13 of the 14 late-onset patients were in mild (CNTNS ⩽ 10) category. CMTNSs and FDSs showed a bimodal distribution in patients with *MFN2* mutations (Fig. 3A and B).

Foot deformities were found in all patients. Pes cavus with flattening was more frequent in the early onset group, and, similarly, high arched foot deformities were more frequent in the late-onset group. Associated signs differed in the early and late-onset groups. Scoliosis (38.5%) and knee joint contracture (26.9%) was found only in patients with an early onset; however, postural hand tremor (30.8%), pain (19.2%) and sensorineural hearing loss (SNHL) (11.5%) were demonstrated by patients with a late onset. In addition, two affected males had bilateral extensor plantar responses with no explanation other than CMT.

Electrophysiological findings

Neurophysiological studies were carried out on 26 affected individuals (11 males and 15 females). MCVs of median, ulnar, peroneal and tibial nerves and SCVs of median, ulnar and sural nerves are shown in Table 3. Electrophysiological findings also confirmed that patients with an early onset were more severely affected than those with a late onset. In the early onset group, the amplitudes of evoked motor responses were often markedly reduced, and we were unable to record amplitudes in 8 of the 12 patients (67%). All patients, except those with absent NCVs, had at least one motor NCV > 38 m/s. However, in the late-onset group, NCVs were obtained for all patients, and some motor

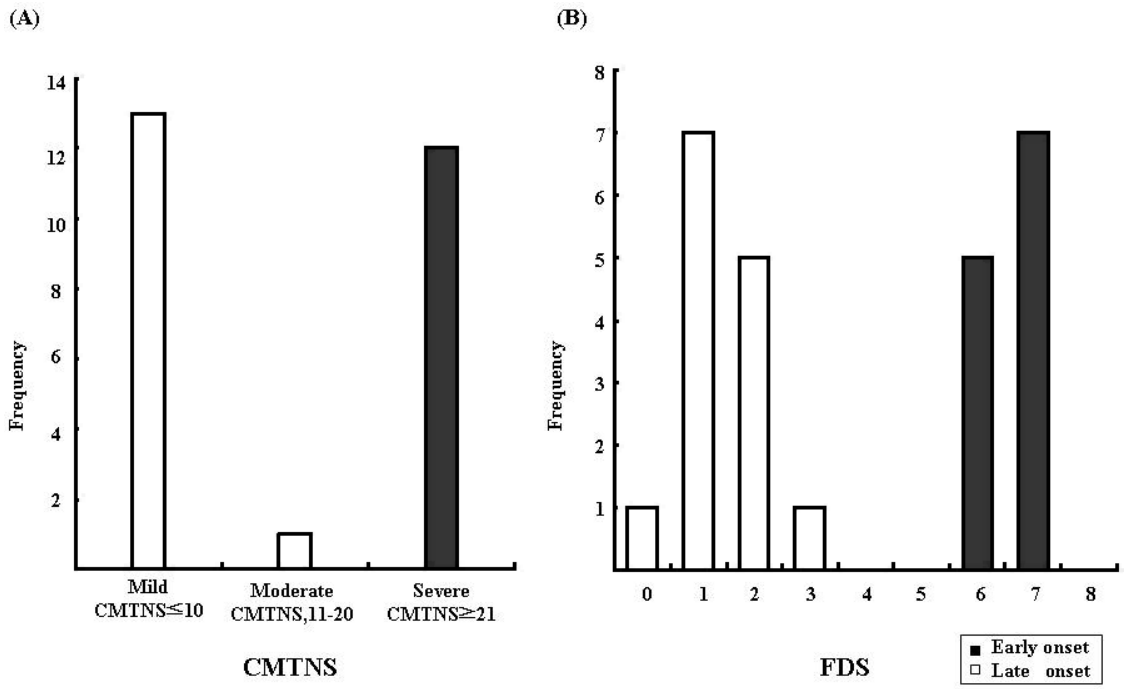

Fig. 3 Quantification of disease severity. Patients with *MFN2* mutations were divided into two categories by onset age (early onset < 10 years or late onset ⩾ 10 years). (**A**) Dimorphic phenotypes of patients with *MFN2* mutations by CMTNS. (**B**) The early onset group was found to be associated with severe functional disability (FDS = 6 or 7) and the late-onset group with asymptomatic to mild disease forms (FDS ⩽ 3).

Table 3 Electrophysiological data in 26 CMT patients from 15 families with *MFN2* mutations

Patient	Age at exam	Motor NCV (m/s)				Sensory NCV (m/s)		
		Median	Ulnar	Peroneal	Tibial	Median	Ulnar	Sural
Early age at onset (<10 years)								
FC1 (II-3)	35	NR	NR	NR	NR	NR	NR	NR
FC1 (III-1)	6	NR	NR	NR	NR	NR	NR	NR
	12	NR	NR	NR	NR	NR	NR	NR
FC1 (III-2)	6	43.7 (2.8)	17.3 (0.2)	NR	NR	NR	NR	NR
	12	NR	NR	NR	NR	NR	NR	NR
FC6 (II-6)	33	NR	NR	NR	NR	NR	NR	NR
FC6 (III-1)	7	NR	NR	NR	NR	NR	NR	NR
	14	NR	NR	NR	NR	NR	NR	NR
FC25 (II-2)	28	40.3 (1.9)	37.3 (2.4)	NR	NR	NR	NR	NR
FC34 (III-2)	4	47.1 (1.2)	48.3 (1.2)	NR	NR	39.6 (29.6)	41.4 (24.8)	NR
	6	40.3 (2.3)	31.1 (0.4)	NR	NR	36.5 (19.6)	33.7 (18.0)	NR
	13	NR	NR	NR	NR	NR	NR	NR
FC55 (II-2)	4	47.2 (7.4)	54.5 (13.0)	NR	NR	22.9 (1.7)	21.7 (1.6)	NR
	6	44.2 (2.4)	38.2 (2.7)	NR	NR	NR	NR	NR
FC87 (II-3)	22	NR	NR	NR	NR	NR	NR	NR
FC87 (III-1)	3	38.9 (1.1)	48.9 (1.5)	37.3 (0.3)	NR	NR	NR	NR
FC113 (II-5)	37	NR	NR	NR	NR	NR	NR	NR
FC113 (III-1)	6	53.8 (10.3)	45.9 (7.4)	NR	NR	NR	NR	NR
Late age at onset (⩾10 years)								
FC48 (II-3)	22	54.5 (11.9)	51.9 (16.6)	34.1 (2.2)	35.2 (0.5)	38.1 (10.4)	34.9 (13.1)	NR
	23	51.1 (12.5)	54.9 (14.1)	36.6 (3.5)	38.2 (0.5)	41.4 (18.4)	45.6 (14.0)	NR
	26	53.2 (12.5)	58.1 (16.5)	35.2 (4.1)	NR	41.4 (8.2)	38.5 (9.2)	NR
FC52 (II-1)	14	50.0 (16.5)	55.7 (19.4)	NR	NR	36.4 (10.0)	36.7 (12.0)	NR
FC70 (II-5)	53	41.2 (10.6)	46.2 (9.6)	37.3 (0.7)	34.7 (0.7)	NR	NR	NR
FC81 (II-5)	60	51.8 (11.5)	50.6 (10.6)	31.4 (0.3)	44.2 (0.2)	40.7 (15.2)	41.5 (14.1)	40.3 (2.6)
	64	51.5 (9.4)	55.1 (9.2)	33.4 (1.2)	NR	38.2 (8.5)	35.0 (11.9)	17.5 (3.4)
FC81 (III-3)	32	46.0 (7.2)	36.4 (2.5)	NR	NR	NR	NR	NR
	35	49.1 (6.5)	38.6 (2.6)	NR	NR	NR	NR	NR
FC111 (III-2)	19	54.0 (20.1)	51.0 (16.6)	41.0 (3.2)	46.0 (6.7)	32.0 (2.8)	31.0 (0.8)	NR
	20	53.0 (19.8)	56.0 (19.0)	42.9 (3.9)	44.7 (8.1)	31.8 (4.0)	31.0 (4.7)	NR
FC135 (III-4)	12	54.8 (12.9)	58.0 (13.0)	NR	25.5 (0.1)	37.5 (9.9)	33.3 (11.2)	NR
FC169 (III-4)	45	57.5 (16.0)	60.3 (16.5)	20.5 (0.1)	NR	36.4 (13.6)	35.5 (14.2)	23.9 (6.1)
FC169 (III-6)	40	58.0 (13.8)	62.5 (14.3)	32.0 (2.3)	47.3 (5.2)	42.9 (22.7)	43.1 (23.4)	36.2 (8.5)
FC169 (III-7)	37	58.3 (18.6)	57.7 (18.4)	17.9 (1.0)	39.3 (0.4)	38.5 (12.1)	37.9 (10.1)	27.7 (2.6)
FC169 (III-8)	52	61.2 (13.4)	63.8 (17.1)	42.8 (1.5)	38.9 (2.4)	39.5 (26.5)	38.0 (17.1)	NR
FC169 (III-12)	38	55.8 (17.8)	57.5 (16.7)	32.5 (1.1)	34.7 (0.5)	39.3 (7.6)	36.3 (7.8)	NR
FC169 (IV-4)	14	56.9 (10.7)	58.6 (6.4)	NR	NR	39.2 (36.9)	37.3 (18.5)	33.7 (9.1)
FC188 (II-2)	43	52.3 (13.6)	58.1 (5.1)	40.7 (5.0)	48.6 (3.5)	29.5 (6.1)	39.3 (5.6)	NR
	46	46.7 (9.2)	58.3 (11.3)	40.7 (4.1)	45.1 (4.3)	25.0 (6.9)	40.9 (7.5)	NR
	49	49.1 (3.4)	22.4 (8.4)	38.4 (2.3)	NR	NR	NR	NR

Amplitudes of evoked responses are given in parentheses (for motor NCVs in mV and for sensory NCVs in μV).
Normal NCV values: motor median nerve = ⩾50.5 m/s; ulnar nerve = ⩾51.1 m/s; tibial nerve = ⩾41.1 m/s; sensory median nerve = ⩾39.3 m/s; ulnar nerve = ⩾37.5 m/s; sural nerve = ⩾32.1 m/s.
Normal amplitude values: motor median nerve = ⩾6 mV; ulnar nerve = ⩾8 mV; tibial nerve = ⩾6 mV; sensory median nerve = ⩾8.8 μV; ulnar nerve = ⩾7.9 μV; sural nerve = ⩾6.0 μV.
NR = not recordable.

NCVs in upper limbs were normal without conduction block. In a patient (III-2 in Family FC34) with an early age at onset, we carried out three follow-up nerve conduction studies over a 10-year period and finally observed the absence of action potentials in all nerves tested (Table 3). Sensory and motor amplitudes changed at a much slower rate in patients with a late onset than in those with an early onset.

The distal and lower limb predominant motor involvement was common in patients with *MFN2* mutations. Therefore, we studied correlations between CMAP and distal limb muscle strength. The amplitudes of the CMAPs of median, ulnar and posterior tibial nerves were found to be significantly correlated with corresponding distal muscle strengths in *MFN2* patients ($r = 0.80$, $P < 0.001$; $r = 0.79$,

$P < 0.001$; $r = 0.78$, $P = 0.005$, respectively). In contrast, the MCVs of median, ulnar and posterior tibial nerves did not correlate with distal muscle strength in *MFN2* patients ($r = 0.50$, $P > 0.05$; $r = 0.48$, $P > 0.05$; $r = 0.58$, $P > 0.05$, respectively). These findings indicate that the weakness is the consequence of axonal loss as reflected in the reduced amplitudes in all motor nerves.

Mean median nerve TLIs in patients with *MFN2* mutations (0.30 ± 0.06, range: 0.16–0.43) were not significantly different from those of 158 healthy controls (0.31 ± 0.04, range: 0.23–0.43). TLIs in the majority of patients in each group were distributed over a narrow range of values. In both early and late-onset groups, TLIs displayed similar distributions (0.30 ± 0.07, range: 0.22–0.43; 0.31 ± 0.06, range: 0.16–0.39, respectively). This finding was expected in CMT2 and supports the hypothesis that axonopathy in patients with *MFN2* mutations is uniformly distributed along nerves.

Ophthalmological findings

Three patients (II-6 and III-1 in Family FC6, and II-3 in Family FC1) developed bilateral optic atrophy during the course of CMT. A patient (II-6 in Family FC6) showed visual impairment at 10 years and experienced a subacute deterioration of visual acuity as low as 20/130 bilaterally. Her son (III-1 in Family FC6) experienced visual deterioration from 13 years and subacute loss of visual acuity as low as 20/100 bilaterally. However, the other patient (II-3 in Family FC1) could not recall the exact age of visual impairment onset and experienced a prolonged decline of visual acuity to as low as 20/200 in the right eye and 20/400 in the left. A central scotoma was detected in all of the above patients. Also, these affected individuals had colour vision defects, and their Ishihara colour plate test results were low (2/21–9/21). Afferent pupillary defect was not found, and intraocular pressures were not increased. Fundus examination of three patients showed a white flat optic disc, attenuation of peripupillary blood vessels and thinning of the retinal nerve fibre layer. The macular, peripheral retina and blood vessels appeared normal, as were the anterior segments of the eye. In addition, one patient (III-1 in Family FC6) had the cup of optic disc showing concentric enlargement and an oval shape. Visual evoked potentials (VEPs) showed no amplitudes in one patient, and markedly reduced amplitudes and delayed patterns in the other patients (Fig. 4A and B). Over the course of several years, both patients in the FC6 family experienced visual acuity recovery to near-normal levels; however, another patient (II-3 in Family FC1) did not improve.

Two daughters of an HMSN VI patient (II-3 in Family FC1) did not have optic atrophy, but extremely severe axonal CMT phenotypes were expressed in both. They showed normal visual acuity (20/20 in both sides) and VEP patterns. Two families (FC55 and FC87) with R364W *MFN2* mutations (like FC1 and FC6) showed normal VEP patterns without optic atrophy (Fig. 4C and D). In addition, two families with R94W, previously reported for HMSN VI, also displayed normal VEP patterns without optic atrophy (Fig. 4E). Moreover, a patient (III-2 in Family FC34) with an early onset with L92P, which showed a clinical course resembling those of R364W or R94W mutations, did not have optic atrophy and normal VEP findings (Fig. 4F). Retinitis pigmentosa was not found in any study subject.

MRI findings

Twenty-one patients with *MFN2* mutations were subjected to brain MRI studies. Eight affected individuals from four families had abnormal MRI findings, namely, T_2 and FLAIR high-signal intensities in centrum semiovale, periventricular and subcortical white matters. The onset age of one patient (II-2 in Family FC55) was earlier than 10 years; however, those of the other seven patients were later. In eight affected individuals, neither hypertension nor diabetes was found.

One patient (II-2 in Family FC55) had confluent periventricular white matter high-signal lesions in right frontal lobe for her age without any other explanation than CMT (Fig. 5A). Moreover, follow-up T_2-weighted MRI scans over 3 years showed no interval change (Fig. 5B). She was born at full period, and no evidence of epileptic seizure, loss of consciousness or behavioural disturbances was documented.

Two patients (III-4 and III-8 in Family FC169) had abnormal brain MRI results in association with transient dysarthria and migraine. Patient III-4 in Family FC169 showed a confluent lesion in the left parietal lobe and multiple non-specific but definitely pathogenic hyperintensities for age (Fig. 6A). She experienced repeated attacks of transient dysarthria persisting for between a few hours and 2 days at the longest. These symptoms recurred at irregular intervals. The other patient (III-8 in Family FC169), the cousin of FC169 (III-4), had similar symptoms. Both experienced migraine without aura.

A patient (II-2 in Family FC188) experienced a sudden attack of transient right upper limb and facial sensory loss for 1 month at 43 years, and, subsequently, experienced recurrent brief transient episodes of paraesthesia with a right upper limb predominance. Brain MRI showed T_1 low, T_2 and FLAIR high-signal intensities in left subcortical lesion without abnormal enhancement (Fig. 6B).

Three patients (III-12 in FC169, and II-5 and III-3 in FC81) harbouring SNHL showed multiple subcortical white matter lesions (Fig. 6C). One patient (II-3 in Family FC48) with bilateral extensor plantar responses also displayed multiple non-specific but pathogenic subcortical hyperintense lesions (Fig. 6D), but an MRI scan of the whole spinal code showed no abnormalities.

Histopathological findings

Sural nerve biopsies were performed in seven patients (*see* Table 2). On light microscopic examination, numbers of myelinated nerve fibres (MNFs) in the early onset group ranged from 2327/mm^2 to 2837/mm^2 (Fig. 7A); however, numbers in

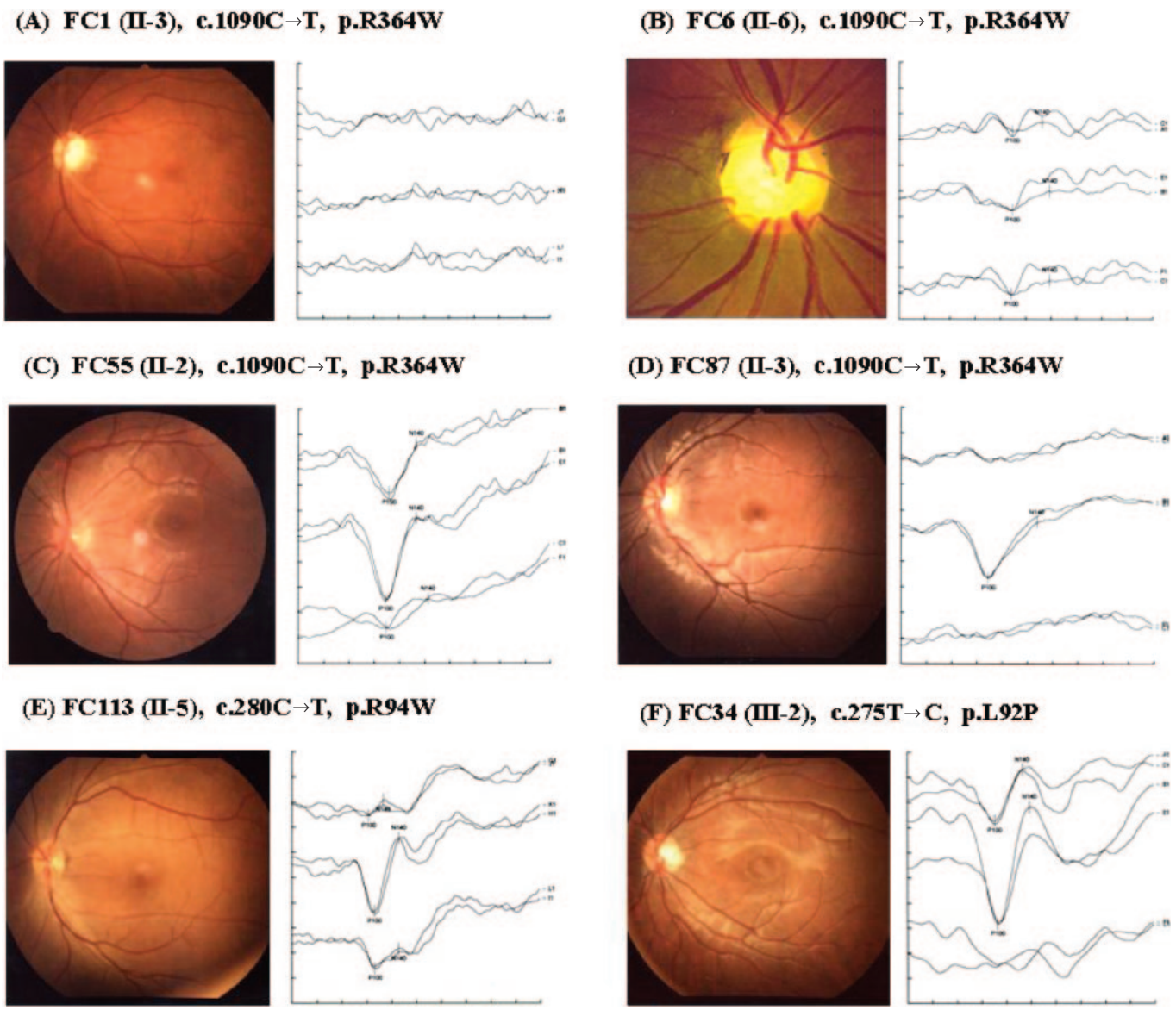

Fig. 4 Fundus examination and VEP in unusually severe patients with early age at onset. (**A**) FC1 (II-3) with R364W showed optic atrophy and no bilateral VEP amplitudes. (**B**) FC6 (II-6) with R364W displayed a white, flat optic disc, and markedly decreased bilateral VEP amplitudes. (**C**) FC55 (II-2) with R364W did not have optic atrophy and showed normal VEP findings. (**D**) FC87 (II-3) with R364W who also did not have optic atrophy and showed normal VEP patterns. (**E**) FC113 (II-5) with R94W, previously reported for HMSN VI, also did not have optic atrophy and displayed normal VEP findings. (**F**) FC34 (III-2) of early onset with L92P showed a very similar clinical course to those with R364W or R94W mutations and had normal VEP findings without optic atrophy.

the late- onset group ranged from 7821/mm^2 to 8356/mm^2 (Fig. 7B). Semi-thin transverse section of the sural nerve showed a marked loss of large myelinated fibres in early onset patients (Fig. 8A), but relatively greater preservation in late-onset patient (Fig. 8B). In both groups, unmyelinated nerve fibres were more preserved than large MNFs; however, those were clustered and atrophied (Fig. 8A). These features are compatible with axonopathy, which is characteristic in CMT2. In one patient (II-3 in Family FC1), the mean number of MNFs was 2299/mm^2, and unmyelinated nerve fibres were relatively better preserved than MNFs. In this patient, diverse features, like pseudo-onion bulb formations that contained more than one axon, were observed by electron microscopy (Fig. 9A and B). One gastrocnemius muscle biopsy was available for histopathological study, in a patient (III-4 in Family FC135) who carried the *MFN2* mutation. This muscle biopsy showed many small grouped atrophic foci, which is characteristic of neurogenic muscle atrophy; however, no ragged-red fibres (RRFs) were observed.

Discussion

In the present study, we identified 10 causative *MFN2* missense mutations in 15 CMT families (24.2%). In particular,

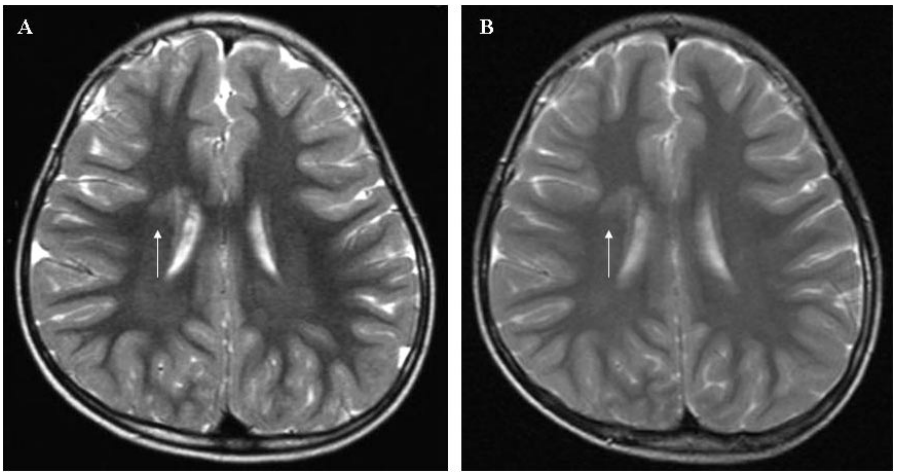

Fig. 5 Transverse T_2-weighted brain MRI showing a confluent hyperintense lesion in the right frontal lobe in Patient FC55 (II-2) with an R364W *MFN2* mutation. The abnormalities observed in T_2-weighted sequences showed no interval change between 3 (**A**) and 6 years of age (**B**).

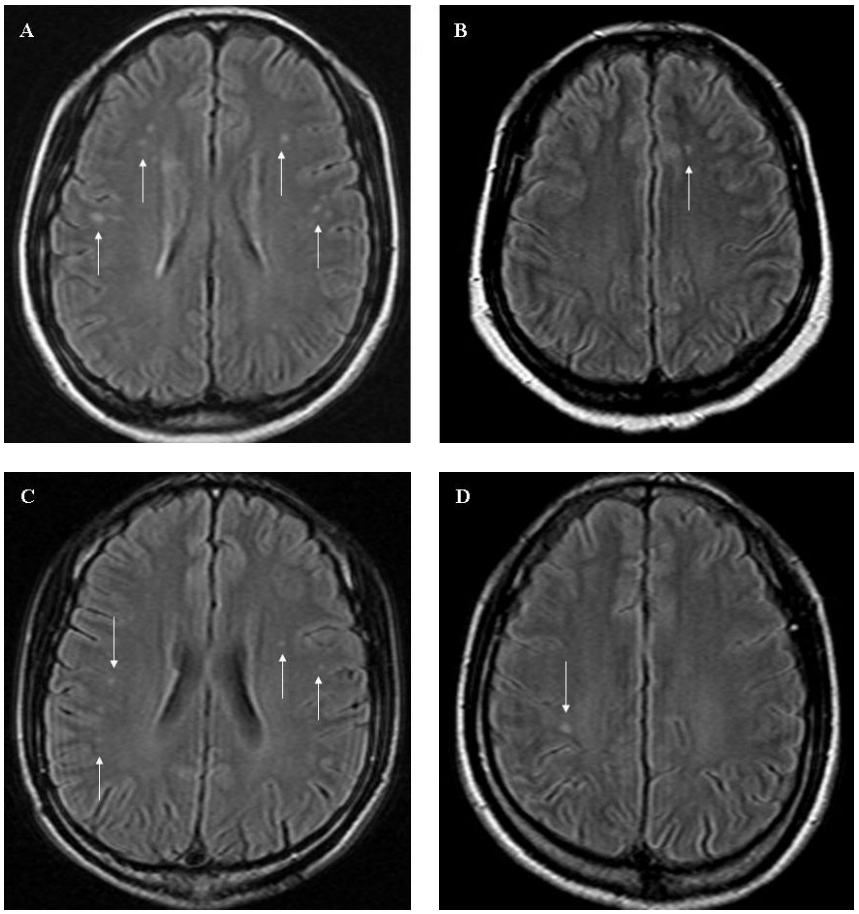

Fig. 6 Transverse FLAIR brain MRI images in patients with MFN2 mutations. (**A**) FC169 (III-4) with transient dysarthria and migraine displayed multiple non-specific but definitely pathogenic subcortical hyperintense lesions. (**B**) FC188 (II-2) having a transient right upper limb and facial sensory loss of 1 month's duration showed T_2 and FLAIR high-signal intensities without abnormal enhancements. (**C**) FC81 (III-3) with H165R showed SNHL and displayed multiple subcortical white matter lesions that could not be attributed to age. (**D**) FC169 (III-7) with R280H showed extensor plantar responses and also demonstrated a non-specific but pathogenic hyperintense lesion.

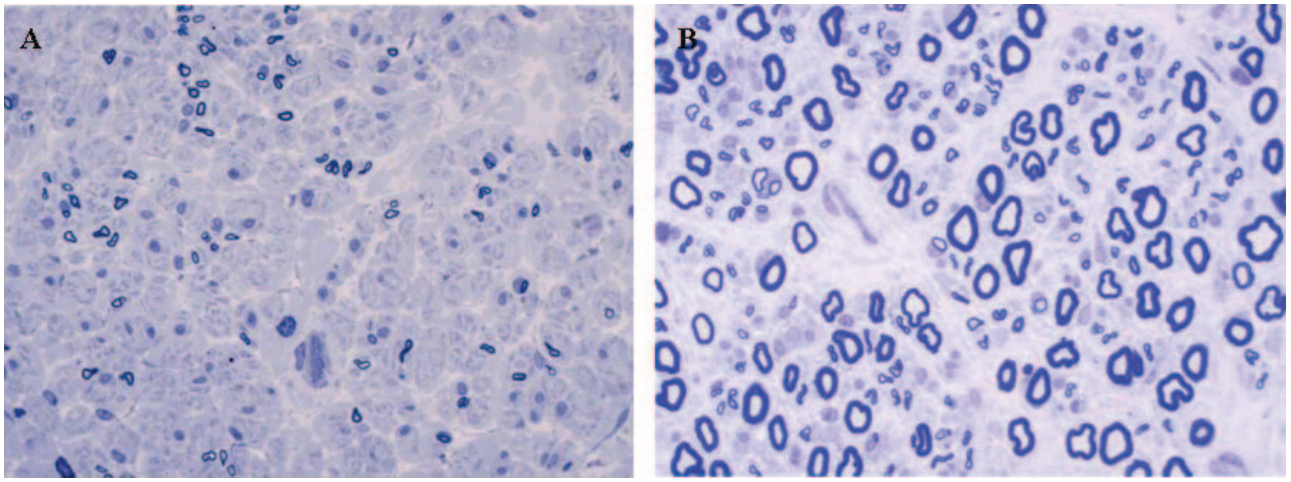

Fig. 7 Light microscopic findings of sural nerve of Patient III-2 in Family FC34 with an early onset (**A**) and of Patient II-2 in Family FC188 with a late onset (**B**). The number of large myelinated fibres was markedly reduced in early onset patient to 2327/mm^2; however, myelinated fibre numbers were relatively well preserved in late-onset patient to 8356/mm^2. Toluidine blue stain. Magnification: **A**, ×400 and **B**, ×400.

six of these mutations were determined to be novel. Mutations observed in the present study involved regions highly conserved between species, for example, *Candida elegans* and *Drosophila melanogaster* (Fig. 1B). All of them cause amino acid substitutions with different properties.

The phenotypic descriptions of the 15 families concur with previous reports and suggest that *MFN2* mutations cause an axonal CMT2 phenotype (Züchner *et al.*, 2004; Kijima *et al.*, 2005; Lawson *et al.*, 2005). In affected individuals with *MFN2* mutations, phenotypes were clearly differentiated into two subgroups. In the early onset group (<10 years), unusually severe phenotypes predominated, whereas in the late-onset group (⩾10 years), most patients had mild phenotypes. Moreover, phenotype severity was also concordant among siblings in individual families, and the clinical courses of families with the same mutations were very similar, indicating that severe and mild phenotypes are determined mainly by the position of mutations in the *MFN2* gene.

In semiological terms, all 12 cases with an early onset required a walker or a wheelchair and were categorized as severe by CMTNS. However, in the late-onset group, one exhibited no disability and the others showed either difficulty walking or an inability to run and were categorized as mild to moderate by CMTNS. Moreover, our electrophysiological findings showed a striking difference between the two subgroups (*see* Table 3). In the early onset group, CMAP amplitudes were markedly reduced, to the extent that CMAPs were not recordable in eight patients (67%). However, in the late-onset group, nerve conductions were recordable in all patients, and some patients presented nearly normal values. In addition, follow-up studies showed that axonal degeneration changes were more rapid in patients with an early onset. Therefore, genetically determined phenotypes were found to correspond well with electrophysiological findings.

It appears that mutational spots with high frequency might exist in *MFN2*, at the 94th, 105th, 280th and 364th codons. In particular, two different missense mutations at the 94th codon have been reported in seven unrelated CMT2A families (four cases of R94W and three cases of R94Q), including two cases in the present study (Züchner *et al.*, 2004, 2006; Kijima *et al.*, 2005). T105M has been detected in three families, once in the present study and once by Züchner *et al.* (2004) and Lawson *et al.* (2005); R280H has also been detected in three families, once in the present study and twice by Züchner *et al.* (2004); whereas R364W has been reported in five families, four unrelated families in the present study and once by Züchner *et al.* (2006).

Population data on *MFN2* mutations by ethnicity are limited, because the relevance of the *MFN2* mutation in CMT2 was reported for the first only recently (Züchner *et al.*, 2004). In the present study, we identified *MFN2* mutations in 24.2% of 62 axonal CMT2 families. Züchner *et al.* (2004) reported 7 (19.4%) mutations in 36 CMT2 families representing several ethnic groups, a Japanese group reported 7 (8.6%) mutations in 81 axonal or unclassified CMT patients (Kijima *et al.*, 2005) and an American study reported 3 (23.1%) mutations in 13 CMT2 families (Lawson *et al.*, 2005). The mutation frequency observed by the Japanese group was lower than those reported by other studies, which may be due to sampling or analytical differences or to different genetic backgrounds. We screened *MFN2* mutations by directly sequencing all exons by PCR in CMT2 patients, whereas Kijima *et al.* (2005) performed denaturing high-performance liquid chromatography (DHPLC) before sequence analysis, which might have reduced the detection rate. In addition, Kijima *et al.* (2005) has reported a case of *de novo* mutation among 7 Japanese CMT2A families with *MFN2* mutations (14.4%);

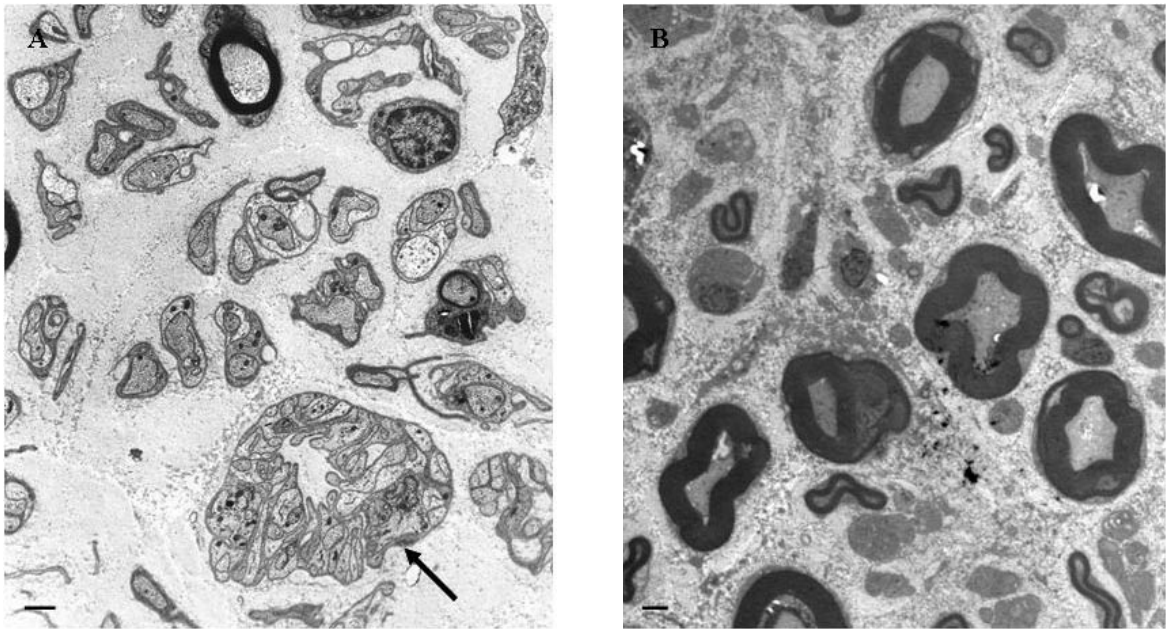

Fig. 8 Sural nerve biopsy of Patient III-2 from Family FC34 with an early onset (**A**) and of Patient II-2 in Family FC188 with a late onset (**B**). (**A**) In electron microscopic findings of sural nerve, unmyelinated nerve fibres were relatively preserved and showed multiple clusters of axonal regeneration (arrow) in early onset patient. (**B**) However, in this figure, large MNFs were more preserved in late-onset patient than in early onset patient. Standard electron microscope techniques are used. Magnification: **A**, ×7080 and **B**, ×2500, Scale bar = 1 μm.

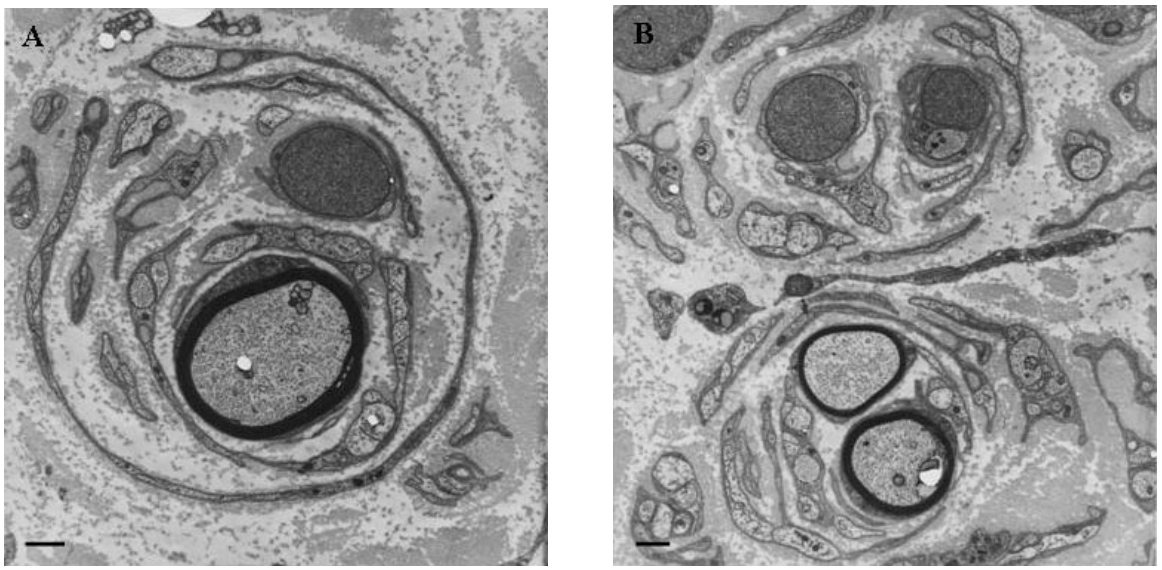

Fig. 9 Sural nerve biopsy of Patient II-3 from Family FC1 with an early onset. Semi-thin transverse section of the sural nerve showing diverse features, such as pseudo-onion bulb formations that contained more than one axon (**A** and **B**) These features may be caused by Schwann cell proliferation in clusters of regenerating nerve fibres. Magnification: **A**, ×10 400 and **B**, ×7080, Scale bar = 1 μm.

however, we could prove *de novo* mutations in at least 5 out of 15 CMT2A families in this study (33.3%). Although additional evidence from other population studies is necessary, we suggest that the frequency of *de novo* mutations may be higher. And, even though a combined analysis of population-based studies on different ethnic groups is not yet available, we believe that *MFN2* mutations are the most common mutation form in axonal CMT.

Electrophysiological evidence indicates that the predominant distal muscle weakness and atrophy of CMT is due to the evolving length-dependent degeneration of motor axons (Hattori *et al.*, 2003). Distally accentuated muscle weakness was found to be strongly correlated with a reduction in the number of functioning large axons, as assessed by CMAPs, but not with nerve conduction slowing. TLI is usually used for determining differential motor conduction slowing

between the distal and proximal segments of a nerve (Dubourg *et al.*, 2001). In the present study, median nerve TLI was the same in controls and in patients with *MFN2* mutations. Moreover, median nerve TLI varied little in controls, or in patients with either an early or late onset, suggesting that axonal degeneration occurring in patients with *MFN2* mutations is homogeneous throughout a given nerve.

Optic atrophy, when noted at the examination of an axonal CMT patient with visual dysfunction, is demonstrated in HMSN VI (Voo *et al.*, 2003). We identified three HMSN VI patients in two unrelated axonal CMT families with R364W mutation. Before molecular diagnosis of *MFN2* gene, all of them were checked for mitochondrial mutations relevant to Leber's hereditary optic atrophy (MIM no. 535000); however, we could not find any mitochondrial mutations. In the FC1 family, children with axonal CMT phenotype did not have visual impairments. Another two families with R364W did not have optic atrophy and two families with R94W, previously reported for HMSN VI, also did not have visual impairments (Züchner *et al.*, 2006). In addition, an early onset patient harbouring L92P mutation, with a clinical course that resembled those with R364W or R94W mutations, did not have optic atrophy. In fact, optic atrophy was only demonstrated by extremely severe axonal CMT patients with an early age at onset, and not by those with a late age at onset. In addition, it has been reported that HMSN VI had variant inherited patterns, and there has been reported an evidence of incomplete penetrance of optic atrophy, whereas the CMT phenotype was expressed in all mutation carriers (Voo *et al.*, 2003; Züchner *et al.*, 2006). Therefore, both the incomplete penetrance and the appearance of optic atrophy in unusually severe patients may be causes of reduced penetrance. On the basis of these findings, we suggest that axonal CMT with optic atrophy harbouring *MFN2* mutation might be a variation of an early onset severe CMT2A phenotype.

The MRI findings of patients with *MFN2* mutations are interesting. We identified a high incidence of CNS involvements in 8 of 21 patients (38%), by brain MRI. Comparing our findings with those of a previous report, which found an increased T_2 signal in both cerebellar peduncles (Züchner *et al.*, 2006), our MRI findings showed T_2 and FLAIR high-signal intensities in centrum semiovale, periventricular and subcortical white matters without abnormal enhancement (*see* Figs 5 and 6). In addition, confluent T_2 hyperintensities were detected in the periventricular white matter of frontal and parietal lobes, and the white matter lesions were considered definitive pathological lesions that could not be attributed to age. In a female patient (II-2 in Family FC55), the abnormalities observed in T_2-weighted sequences showed no interval change between 3 and 6 years of age, which differs from the findings of cerebral lesions in unusual CMTX (CMT neuropathy type X) cases associated with transient CNS abnormalities, in which such changes are reversible over a relatively short period (Paulson *et al.*, 2002; Hanemann *et al.*, 2003). Subclinical CNS involvement in patients with Cx32 mutations has been previously reported (Nicholson *et al.*, 1998; Bahr *et al.*, 1999). We also found subclinical CNS involvements in patients with *MFN2* mutations. In addition, abnormal MRI findings were more common in the late-onset group; therefore, we considered that these were not necessarily associated with age at onset or clinical severity. Moreover, it would be of interest to determine whether these non-specific but pathogenic findings are also found frequently in other populations with *MFN2* mutations.

However, the relation between these abnormal brain MRI findings and mitochondrial dysfunction due to *MFN2* mutations has not been established. The possible explanation for white matter changes in brain MRI findings of our patients is that MFN2 is highly abundant in brain, and it has been well known that mitochondria play a pivotal role in coordinating programmed cell death; therefore, while numerous cell death pathways are activated following an episode of brain ischaemia, mitochondrial dysfunction appears to be a crucial factor in the life or death decision (Fiskum *et al.*, 2000; Zipfel *et al.*, 2000; Bach *et al.*, 2005; Korde *et al.*, 2005). Whatever the exact pathomechanism turns out to be, it is important to remember that there are clinical examples of CNS involvements.

MFN2 mutations have been associated with clinical findings suggesting CNS involvement. CMT with a pyramidal feature is an axonal form of CMT with variable pyramidal features but without frank spasticity (Vucic *et al.*, 2003). In the present study, extensor plantar responses were found in one patient (II-3 in Family FC48) and brain and spine MRI findings were normal; however, the other patient (III-7 in Family FC169) with extensor plantar responses had an abnormal brain MRI. Both of these patients had flexor plantar weakness and increased knee and ankle reflexes but no frank spasticity, which is differentiated from spastic paraplegia. These findings are similar to the previous report by Zhu *et al.* (2005). In addition, SNHL was found in three patients with H165R and M376T mutations; all three cases had multiple subcortical hyperintense lesions on brain MRI. Although the additional evidences from *in vivo* or *in vitro* studies are necessary, we suggest that *MFN2* mutations may cause variable CNS involvements.

Nerve biopsy findings in CMT2A patients showed typical evidence of axonopathy, such as axonal cluster formation, atrophy and loss of thick MNFs, as is found in CMT2 (Berciano *et al.*, 1986; Thomas *et al.*, 1996). The mean number of myelinated fibres in patients with an early onset was reduced by 70% compared with that in patients with a late onset. However, unmyelinated nerve fibres were similarly well preserved in both groups (*see* Figs 7 and 8). In a patient (II-3 from Family FC1), an electron microscopic examination showed some pseudo-onion bulb formations (*see* Fig. 9), and it would appear that this feature may have been caused by Schwann cell proliferation in clusters of regenerating nerve fibres.

Mutations in *MFN2* gene are now viewed as the primary cause of axonal autosomal dominant CMT2A, and, thus, it

has been suggested that *MFN2* should be screened for in these patients. However, clinical and electrophysiological phenotypes of CMT patients with *MFN2* mutations were significantly different in early and late disease-onset groups, and optic atrophy was found only in CMT2 patients with unusually severe phenotypes with an early age at onset. In addition, *MFN2* mutations show variable CNS involvements. On the basis of prior evidence and the present study, it seems probable that *MFN2* mutations affect the nervous system at various levels, and that HMSN VI might be a variant of an early onset severe CMT2A phenotype.

Acknowledgements

We wish to thank Dr M. Shy for critical review of this manuscript. This work was supported by a grant of the Korea Health 21 R&D Project, Ministry of Health and Welfare, Korea (A05-0503-A20718-05N1-00010A), and in part by the Brain Korea 21 project, Ministry of Education.

References

Antonellis A, Ellsworth RE, Sambuughin N, Puls I, Abel A, Lee-Lin SQ, et al. Glycyl tRNA synthetase mutations in Charcot-Marie-Tooth disease type 2D and distal spinal muscular atrophy type V. Am J Hum Genet 2003; 72: 1293–9.

Bach D, Naon D, Pich S, Soriano FX, Vega N, Rieusset J, et al. Expression of MFN2, the Charcot-Marie-Tooth neuropathy type 2A gene, in human skeletal muscle: effects of type 2 diabetes, obesity, weight loss, and the regulatory role of tumor necrosis factor alpha and interleukin-6. Diabetes 2005; 54: 2685–93.

Bahr M, Anders F, Timmerman V, Nelis ME, Van Broeckhoven C, Dichgans J. Central visual, acoustic, and motor pathway involvement in a Charcot-Marie-Tooth family with an Asn205Ser mutation in the connexin 32 gene. J Neurol Neurosurg Psychiatry 1999; 66: 202–6.

Berciano J, Combarros O, Figols J, Calleja J, Cabello A, Silos I, et al. Hereditary motor and sensory neuropathy type II. Clinicopathological study of a family. Brain 1986; 109: 897–914.

Birouk N, LeGuern E, Maisonobe T, Rouger H, Gouider R, Tardieu S, et al. X-linked Charcot-Marie-Tooth disease with connexin 32 mutations: clinical and electrophysiologic study. Neurology 1998; 50: 1074–82.

Bissar-Tadmouri N, Nelis E, Züchner S, Parman Y, Deymeer F, Serdaroglu P, et al. Absence of KIF1B mutation in a large Turkish CMT2A family suggests involvement of a second gene. Neurology 2004; 62: 1522–5.

Boerkoel CF, Takashima H, Garcia CA, Olney RK, Johnson J, Berry K, et al. Charcot-Marie-Tooth disease and related neuropathies: mutation distribution and genotype-phenotype correlation. Ann Neurol 2002; 51: 190–201.

Chen H, Detmer SA, Ewald AJ, Griffin EE, Fraser SE, Chan DC. Mitofusins Mfn1 and Mfn2 coordinately regulate mitochondrial fusion and are essential for embryonic development. J Cell Biol 2003; 160: 189–200.

Chen H, Chomyn A, Chan DC. Disruption of fusion results in mitochondrial heterogeneity and dysfunction. J Biol Chem 2005; 280: 26185–92.

Choi BO, Lee MS, Shin SH, Hwang JH, Choi KG, Kim WK, et al. Mutational analysis of PMP22, MPZ, GJB1, EGR2 and NEFL in Korean Charcot-Marie-Tooth neuropathy patients. Hum Mutat 2004; 24: 185–6.

De Jonghe P, Timmerman V, Broeckhoven CV. Workshop Participants. 2nd Workshop of the European CMT Consortium: 53rd ENMC International Workshop on Classification and Diagnostic Guidelines for Charcot-Marie-Tooth Type 2 (CMT2HMSN II) and Distal Hereditary Motor Neuropathy (Distal HMNSpinal CMT): 26-28 September 1997, Naarden, The Netherlands. Neuromusc Disord 1998; 8: 426–31.

Dubourg O, Tardieu S, Birouk N, Gouider R, Leger JM, Maisonobe T, et al. Clinical, electrophysiological and molecular genetic characteristics of 93 patients with X-linked Charcot-Marie-Tooth disease. Brain 2001; 124: 1958–67.

Evgrafov OV, Mersiyanova I, Irobi J, Van Den Bosch L, Dierick I, Leung CL, et al. Mutant small heat-shock protein 27 causes axonal Charcot-Marie-Tooth disease and distal hereditary motor neuropathy. Nat Genet 2004; 36: 602–6.

Fiskum G. Mitochondrial participation in ischemic and traumatic neural cell death. J Neurotrauma 2000; 17: 843–55.

Hanemann CO, Bergmann C, Senderek J, Zerres K, Sperfeld AD. Transient, recurrent, white matter lesions in X-linked Charcot-Marie-Tooth disease with novel connexin 32 mutation. Arch Neurol 2003; 60: 605–9.

Hattori N, Yamamoto M, Yoshihara T, Koike H, Nakagawa M, Yoshikawa H, et al. Demyelinating and axonal features of Charcot-Marie-Tooth disease with mutations of myelin-related proteins (PMP22, MPZ and Cx32): a clinicopathological study of 205 Japanese patients. Brain 2003; 126: 134–51.

Honda S, Aihara T, Hontani M, Okubo K, Hirose S. Mutational analysis of action of mitochondrial fusion factor mitofusin-2. J Cell Sci 2005; 118: 3153–61.

Iwashita H, Inoue N, Araki S, Kuroiwa Y. Optic atrophy, neural deafness, and distal neurogenic amyotrophy. Arch Neurol 1970; 22: 357–64.

Kijima K, Numakura C, Izumino H, Umetsu K, Nezu A, Shiiki T, et al. Mitochondrial GTPase mitofusin 2 mutation in Charcot-Marie-Tooth neuropathy type 2A. Hum Genet 2005; 116: 23–7.

Korde AS, Pettigrew LC, Craddock SD, Maragos WF. The mitochondrial uncoupler 2,4–dinitrophenol attenuates tissue damage and improves mitochondrial homeostasis following transient focal cerebral ischemia. J Neurochem 2005; 94: 1676–84.

Koshiba T, Detmer SA, Kaiser JT, Chen H, McCaffery JM, Chan DC. Structural basis of mitochondrial tethering by mitofusin complexes. Science 2004; 305: 858–62.

Krauss W. Atrophia nervi optici and neurotische Muskelartophie. Z Augenheilk 1906; 16: 503–16.

Lawson VH, Graham BV, Flanigan KM. Clinical and electrophysiologic features of CMT2A with mutations in the mitofusin 2 gene. Neurology 2005; 65: 197–204.

Mersiyanova IV, Perepelov AV, Polyakov AV, Sitnikov VF, Dadali EL, Oparin RB, et al. A new variant of Charcot-Marie-Tooth disease type 2 is probably the result of a mutation in the neurofilament-light gene. Am J Hum Genet 2000; 67: 37–46.

Muglia M, Zappia M, Timmerman V, Valentino P, Gabriele AL, Conforti FL, et al. Clinical and genetic study of a large Charcot-Marie-Tooth type 2A family from Southern Italy. Neurology 2001; 56: 100–3.

Nicholson GA, Young I, Corbett A. Efficient neurophysiologic selection of X-linked Charcot-Marie-Tooth families: ten novel mutations. Neurology 1998; 51: 1412–6.

Pareyson D. Differential diagnosis of Charcot-Marie-Tooth disease and related neuropathies. Neurol Sci 2004; 25: 72–82.

Paulson HL, Garbern JY, Hoban TF, Krajewski KM, Lewis RA, Fischbeck KH, et al. Transient central nervous system white matter abnormality in X-linked Charcot-Marie-Tooth disease. Ann Neurol 2002; 52: 429–34.

Rojo M, Legros F, Chateau D, Lombes A. Membrane topology and mitochondrial targeting of mitofusins, ubiquitous mammalian homologs of the transmembrane GTPase Fzo. J Cell Sci 2002; 115: 1663–74.

Rosenberg RN, Chutorian A. Familial opticoacoustic nerve degeneration and polyneuropathy. Neurology 1967; 17: 827–32.

Schneider DE, Abeles MM. Charcot-Marie-Tooth disease with primary optic atrophy: report of two cases occurring in two brothers. J Nervous Mental Dis 1937; 85: 541–7.

Shy ME. Charcot-Marie-Tooth disease: an update. Curr Opin Neurol 2004; 17: 579–85.

Shy ME, Blake J, Krajewski K, Fuerst DR, Laura M, Hahn AF, et al. Reliability and validity of the CMT neuropathy score as a measure of disability. Neurology 2005; 64: 1209–14.

Szigeti K, Garcia CA, Lupski JR. Charcot-Marie-Tooth disease and related hereditary polyneuropathies: molecular diagnostics determine aspects of medical management. Genet Med 2006; 8: 86–92.

Tang BS, Zhao GH, Luo W, Xia K, Cai F, Pan Q, et al. Small heat-shock protein 22 mutated in autosomal dominant Charcot-Marie-Tooth disease type 2L. Hum Genet 2005; 116: 222–4.

Thomas PK, King RH, Small JR, Robertson AM. The pathology of Charcot-Marie-Tooth disease and related disorders. Neuropathol Appl Neurobiol 1996; 22: 269–84.

Verhoeven K, De Jonghe P, Coen K, Verpoorten N, Auer-Grumbach M, Kwon JM, et al. Mutations in the small GTPase late endosomal protein RAB7 cause Charcot-Marie-Tooth type 2B neuropathy. Am J Hum Genet 2003; 72: 722–7.

Vizioli F. Dell's atrofia muscolare progressive nervrotica. Boll de la R Accad Med-Chir, 1889.

Voo I, Allf BE, Udar N, Silva-Garcia R, Vance J, Small KW. Hereditary motor and sensory neuropathy type VI with optic atrophy. Am J Ophthalmol 2003; 136: 670–7.

Vucic S, Kennerson M, Zhu D, Miedema E, Kok C, Nicholson GA. CMT with pyramidal features. Charcot-Marie-Tooth. Neurology 2003; 60: 696–9.

Zhao C, Takita J, Tanaka Y, Setou M, Nakagawa T, Takeda S, et al. Charcot-Marie-Tooth disease type 2A caused by mutation in a microtubule motor KIF1B beta. Cell 2001; 105: 587–97.

Zhu D, Kennerson ML, Walizada G, Zuchner S, Vance JM, Nicholson GA. Charcot-Marie-Tooth with pyramidal signs is genetically heterogeneous: families with and without *MFN2* mutations. Neurology 2005; 65: 496–7.

Zipfel GJ, Babcock DJ, Lee JM, Choi DW. Neuronal apoptosis after CNS injury: the roles of glutamate and calcium. J Neurotrauma 2000; 17: 857–69.

Züchner S, Mersiyanova IV, Muglia M, Bissar-Tadmouri N, Rochelle J, Dadali EL, et al. Mutations in the mitochondrial GTPase mitofusin 2 cause Charcot-Marie-Tooth neuropathy type 2A. Nat Genet 2004; 36: 449–51.

Züchner S, De Jonghe P, Jordanova A, Claeys KG, Guergueltcheva V, Cherninkova S, et al. Axonal neuropathy with optic atrophy is caused by mutations in mitofusin 2. Ann Neurol 2006; 59: 276–81.